Shegokar and Singh, 1:3
http://dx.doi.org/10.4172/scientificreports.192

Open Access Scientific Reports

Research Article Open Access

Preparation, Characterization and Cell Based Delivery of Stavudine Surface Modified Lipid Nanoparticles

Ranjita Shegokar[1,2]* and Kamalinder K. Singh[1]

[1]S.N.D.T. Women's University, C. U. Shah College of Pharmacy, , Santacruz (W), Mumbai 400049, India
[2]Freie Universität Berlin, Institute of Pharmacy, Department Pharmaceutics, Biopharmaceutics & NutriCosmetics, Kelchstraße 31, Berlin, Germany

Abstract

Previously it was shown that uncoated lipid nanoparticles of stavudine proved effective in targeting HIV viral sites in body. Therefore, the main objective of this work was to prepare and characterize surface modified stavudine entrapped lipid nanoparticles as potential drug delivery system for anti-HIV chemotherapy. The physical, targeting potential (both *in vitro* and *in vivo*) and toxicological evaluation was performed on developed nanocarriers. The degree of targeting and cellular uptake demonstrated differences among the surface coated lipid nanoparticles. We found that developed lipid nanoparticles are easy to prepare using high pressure homogenization, and has excellent stability at room temperature and refrigeration condition. In future, developed surface modified lipid nanoparticles can be evaluated clinically.

Keywords: HIV/AIDS; Stavudine; Solid lipid nanoparticles (SLN); Cellular uptake and organ targeting

Introduction

A major barrier to successful HIV therapy via nanoparticles poses a challenge of delivering the drug at target site like spleen, brain, bone marrow etc. with optimized particle size for extended duration of time with minimized toxicity [1,2]. This could be achieved by targeting anti-retrovirals encapsulated in lipid or polymeric nanoparticles. Nanoparticles based on solid lipids can greatly improve the solubilization and the bioavailability of therapeutic molecules by easily penetrating to cellular viral reservoirs [3-5]. Surface characteristics and size are the major determinants of the clearance kinetics and biodistribution of colloidal lipid particles. Also in order to achieve an active targeting towards specific tissues, selective ligands have to be attached to the nanoparticle surface to enable molecular recognition [6]. However, chemical coupling of such ligands is often difficult, because of the absence of reactive groups at the surface of carriers. In this work, the selective retention of lipid nanoparticles (10-250 nm) in anatomical or cellular reservoirs is expected to provide better targeting. Due to lipophilic composition, feasibility of production of ultrafine size nanoparticles, solid lipid nanoparticles (SLNs) can be used as carrier for delivering anti-retroviral drug.

Literature reports modification of nanoparticle surface using different molecular weight poly-ethylene glycol (PEG)[7], folic acid [8], asialoglycoproteins, poloxamer 407, poloxamine 908 [9], Tween 80 [10], lectins [11,12], heparin [13], albumin [14,15] and polysaccharides [16]. Polysaccharide coatings have been considered as an alternative to the other coatings, as additionally, they have specific receptors in certain cells or tissues which are involved in tissue addressing and transport mechanisms [17]. Beside this, polysaccharides constitute an important class of physiological materials and possess well reported biocompatibility and biodegradability. It has already been demonstrated that lectins play an important role in biological recognition events and can bind to intestinal mucosa and facilitate transport across cellular barriers [18].

The main objective of present work was to develop a new surface modified macrophage specific drug delivery platform for antiretroviral therapy. For this purpose, stavudine encapsulated lipid nanoparticles were prepared, surface modified and characterized in comparison with uncoated lipid nanoparticles. *In vitro* cellular uptake and cytotoxicity studies were conducted in primary macrophages to get idea about cellular behavior of prepared nanoparticles. Finally, nanoparticles were radiolabelled and their pharmacokinetic and biodistribution profile in rats was studied.

Material and Methods

Stavudine (Alkem Laboratories, Mumbai, India), dynasan 114 (Sasol GmbH, Hamburg, Germany), Solutol HS 15 (Sasol GmbH, Hamburg, Germany), Plurol® Oleique CC 497 (Gattefossé, France), Poloxamer 188 (BASF Inc., NJ, USA) and Tween 80 (S. D. Fine Chemicals, Mumbai, India), dextran (Pharmacosmos A/S, Holbaek, Denmark) were received as free sample. RPMI medium (Roswell Park Memorial Institute), fetal calf serum (FCS), bovine serum albumin, hanks buffered salt solution (HBSS), yellow MTT (3-(4,5-Dimethylthiazol-2-yl)-2,5-diphenyltetrazolium bromide, a tetrazole), Dulbecco's modified eagle medium (DMEM) were purchased from Hi Media, Mumbai, India. Diethylene triamine penta acetic acid (DTPA), dimethyl sulfoxide (DMSO), polyethylene glycol 1000 and stanneous chloride ($SnCl_2$) were purchased from S. D. Fine Chemicals, Mumbai, India.

Experimental

Preparation of uncoated (bare) nanoparticles: Lipid nanoparticles were prepared using hot high pressure homogenization technique employing dynasan 114 as lipid matrix. The drug was dissolved in melted lipid containing mixture of hydrophobic surfactants (Solutol

***Corresponding author:** Ranjita Shegokar, Freie Universität Berlin, Institute of Pharmacy, Department Pharmaceutics, Biopharmaceutics & NutriCosmetics, Kelchstraße 31, Berlin, Germany, Tel: +49-30-83850624; Fax: +49-30-83850616; E-mail: ranjita@arcsindia.com

Received March 15, 2012; **Published** July 28, 2012

Citation: Shegokar R, Singh KK (2012) Preparation, Characterization and Cell Based Delivery of Stavudine Surface Modified Lipid Nanoparticles. 1: 192. doi:10.4172/scientificreports.192

1%, Tween 80 1%, Plurol Oleique 1%, w/w) and slowly dispersed in 0.5% aqueous solution of Poloxamer 188 at 80 ± 2°C. The formed pre-emulsion was then passed through high pressure homogenizer (APV 2000 lab model) at different pressures of 200, 600 and 800 bar.

Preparation of coated (surface modified) nanoparticles: To enhance the targeting potential of bare lipid nanoparticles (NP), the surface of nanoparticle was modified using 1% w/w concentration of each polyethylene glycol 1000 (batch PNP), serum albumin (batch BNP), and dextran 60 (batch DNP) individually by incubating at 37 ± 2°C for 12h. Adsorption of the polymers onto the surface of nanoparticles was confirmed by measuring increase in the particle size and atomic force microscopy.

Characterization of surface modified lipid nanoparticles (SM-NP): The stavudine nanoparticles were observed for any sign of instability, color, odor change, creaming or sedimentation and pH of all the batches was determined using calibrated Remi pH meter. Particle size determination in distilled water using photon correlation spectroscopy (PCS) and laser diffractometry was performed. The zeta potential determination and TEM analysis was performed as discussed in our previous paper [19].

Atomic force microscopy analysis (AFM): AFM analysis was performed at room temperature on silanized mica surface for bare and surface modified lipid nanoparticles. The nanoparticles (40µl) were deposited onto a small mica disk (diameter of 1 cm). After 2 min, the excess of dispersion was removed using paper filter. The AFM images in tapping mode (Veeco Digital Instruments Multimode Nanoscope IV) were recorded at spring constant of 30-80 N/m and resonance frequency of ~340 kHz. ProScan Data Acquisition software developed under Windows 95 was used for further image analysis.

Phagocytic uptake studies

Phagocytic uptake studies were performed on primary peritoneal macrophages harvested from male Wister rats. The lavaged macrophage cell suspension was centrifuged at 1300 rpm at 4°C, and the sediment was re-suspended in HBSS. The suspension was used to form monolayer on glass cover slips in presence of RPMI 1640 supplemented with 10% FCS at 37°C ± 2°C in sterilized culture plates. After 3h, medium was exchanged with NP and SM-NP labeled with Rhodamine 123. The pure rhodamine solution was used as blank and phosphate buffer saline (PBS, pH 7.4) as control. The culture plates were incubated at 37°C ± 2°C/5% CO_2. The uptake was arrested at specific time intervals by immersing the plate in an ice bath. Olympus fluorescence microscope at excitation and emission wavelengths of 507 and 529 nm was used. To assess the qualitative determination in comparison to plain dye, cells were separated from medium by centrifugation (2000 rpm/ 15 min) and lysed using hypotonic saline. The fluorescence associated with the supernatant recovered from nanoparticles harvested cells was determined using fluorimetry ($\lambda_{excitation}$ 485 nm/ $\lambda_{emission}$ 529 nm). The percent cellular uptake was calculated using following formula in triplicates.

$$\text{Uptake efficiency}\,(\%) = (W_{sample} / W_{total}) \times 100\%$$

where, W_{sample} is the amount of Rhodamine 123 associated with macrophage cells, and W_{total} is the total amount of Rhodamine 123 present in the feed nanoparticle.

Cytotoxicity

The cell toxicity was performed using MTT assay in murine macrophages J774.A12 cultured at 1x105 (National Centre for Cell Sciences, Pune, India) and treated with lipid nanoparticles of stavudine for 6 h at 37° ± 2°C/5% CO_2. After 6h incubation, MTT reaction was terminated by addition of acid propanol (1M HCl: isopropanol in 1:24 ratio) and the absorbance of converted dye was measured spectrophotometrically at 570 nm. The % cytotoxicity (n=3) was calculated using following formula,

$$\%\ \text{Cytotoxicity} = \frac{(100 - \text{Optical density}_{PBS})}{(\text{Optical density}_{PBS}) - (\text{Optical density}_{TEST})} \times 100$$

In vivo experiments

A 24 h study was performed to access pharmacokinetic and biodistribution pattern of radiolabelled SM-NP. Lipid nanoparticles were injected in rats intravenously via tail vein after anesthetization using 1:1 mixture of ketamine (10% w/v) and xylazine (2% w/v). All the rats were received single dose of 2.7 mg/kg 99mTc labeled (1.2 mCi) stavudine drug solution (STV-DS) and lipid nanoparticles (NP, PNP, BNP, and DNP). Gamma scintigraphic images were captured using Millennium MPS Acquisition System, Multi Purpose Single Head, square detector gamma camera (General Electrical, U.S.A) and processed by eNTEGRA work station. At stipulated time intervals of 5, 15, 30, 45 min, 1, 4, 8 and 24 h blood was collected from retro-orbital puncture using a fine glass capillary into a small glass test tube containing 0.3% sodium citrate solution. For biodistribution studies at end of 1, 4, 8 and 24 h, the animals were humanly sacrificed using inhalation of high amount of anesthetic ether. The rats were dissected and major tissues like brain, lung, liver, kidney, spleen, heart and thymus were removed and washed with Ringer's solution to remove any adherent debris and dried using tissue paper. The organs were weighted and triturated to form homogenate. Radioactivity corresponding to one gram of organ homogenate or blood was measured using well-type gamma scintillation counter and expressed as injected dose (ID) per gram of organ. Pharmacokinetic parameters like Cmax, Tmax, area under zero-moment curve (AUC), area under first-moment curve (AUMC), mean residence time (MRT) were calculated using GraphPad Prism software (version 4.03, USA). All the results are expressed as the mean ± SD and statistical analysis was assessed using student's t-test with $p < 0.05$ as the minimum level of significance.

The radiolabelling conditions for lipid nanoparticles were optimized for pH (5, 6, 7, and 8), time of incubation (0, 5, 15, 30 and 45 min) and $SnCl_2$ (50, 250, 500, 1000µg and 2500µg/ml) concentrations. *In vitro* stability of radiocomplex in PBS (pH 7.4) and plasma for NP and SM-NP was also studied. In another experiment, the stability and strength of complexation of 99mTc with lipid nanoparticles was challenged against various concentrations of DTPA at 0.05%, 0.5%, 1% and 2% after 2 h incubation and the effect on labeling efficiency was studied using thin layer chromatography, details can be found in our previously published paper. All animal studies were approved by Institutional Animal Ethical Committee of Bombay Veterinary College, Nuclear Medicine Department, Mumbai, India.

Toxicity studies

Toxicity profile of STV-DS, blank NP (BL-NP), NP and DNP was checked in albino Wister rats for acute and repeated dose. The animals

were given free access to water 2h after the treatment but denied food for 8h prior to treatment. In acute toxicity study, test substances (90 mg/kg dose) were administered intravenously (IV) in divided doses over a period of 24h. One animal group was maintained as untreated/control. All animals were observed up to 14 days after treatment for mortality and abnormal behavior. For repeated dose toxicity study, the doses (3.6 mg/kg/day of stavudine) were administered intravenously daily over a period of 14 days. The effect of the treatment on important physiological functions of animals such as locomotion, behavior, respiration and pharmacologic signs like convulsions and vomiting were noted for all the experimental animals over period of 28 days. Observation for mortality was also made. All the animals in each of the experimental groups were humanly sacrificed using inhalation of high amount of anesthetic ether at the end of 14 days (acute dose toxicity) and 28 days (repeated dose toxicity) and organ of interest were collected and checked for any histopathological changes.

Results and Discussion

Preparation and characterization of bare and surface modified lipid nanoparticles

The trimyristin loaded uncoated lipid nanoparticles produced using hot high pressure homogenization showed decrease in particle size with increase in homogenization pressure up to 800 bars (77 nm). The mean particle size after 2 cycles at 200 bars was 75 nm and had polydispersity index of 0.120 [19] which almost remained constant even at 800 bars. Laser diffractometry confirmed the results obtained with photon correlation spectroscopy. The same lipid nanoparticle batch was successfully scaled up to 0.5 ton using different capacity homogenizers at optimized production conditions [20]. The stavudine lipid nanoparticles were also successfully converted into dry powder form using different cryoprotectants making them suitable for IV administration [21]. The drug content of lipid nanoparticles of stavudine was found to be around 96%. In present work, surface of lipid nanoparticle was modified for making them more selective in targeting the drug to specific site in body. An attempt was made to modify the surface of nanoparticles by physical adsorption. Dextran 40, 60 and 70, bovine serum albumin and PEG 1000 were used as surface modifier.

All dextrans were tried at concentration of 0.1, 1 and 2% w/w. The increase in particle size observed was 78 to 85 nm from initial size of 75 nm. The physical adsorption of dextran 40 was found to be more effective when used at higher concentration i.e. 2% w/w. Adsorption increased with increase in concentration of dextran which further led to increase in particle size. The particle size increase at 1% and 2% w/w concentration was almost comparable. The dextran 60 gave highest surface adsorption at 1% w/w concentration forming layer around the particle surface of thickness 10-12 nm. Lipid nanoparticles when incubated with dextran 60 at 0.1 and 2% w/w showed slight increase in particle size and polydispersity index. Dextran 70 showed highest physical adsorption at lower concentration with increase in particle size of 6-7 nm, but within 2 days the particle growth was observed. Among all dextran tried, dextran 60 gave stable and reproducible increase in particle size at 1%w/w concentration.

Albumin, as plasma protein when ionized is negatively charged, it is essential for maintaining the osmotic pressure needed for proper distribution of body fluids between intravascular compartments and body tissues [22]. It also acts as a plasma carrier by non-specifically binding several hydrophobic steroid hormones and as a transport protein. The stavudine lipid nanoparticles were coated with serum albumin at 0.25, 0.5 and 1% w/w concentration. After 24 h incubation, BSA gave particle size increase from 75 to 93 nm. At lower concentration of BSA i.e. 0.25 and 0.5% w/w the particle size increased to 81 to 83 nm, respectively. The nanoparticles almost had 5 to 20 nm increase in mean particle size after physical adsorption of serum albumin (1%w/w).

Four different types of polyethylene glycols (PEG 300, 400, 600 and 1000) were tried as surface modifier. The PEG 300, 400 and 600 did not show any increase in particle size of stavudine lipid nanoparticles when used at 2, 5 and 10% w/w concentration, indicating the absence of surface modification or PEGylation. The concentration dependant increase in particle size was observed for PEG 1000 (0.25, 0.5 and 1%). At lower concentration of 0.25% w/w, the particle size of nanoparticles was found to increase by 9-10 nm whereas at higher concentration of 0.5% it showed 28-30 nm increase in particle size. This difference was quite significant from the initial particle size of lipid nanoparticles. The PEG at higher concentration of 1% showed highest physical adsorption leading to an increase in particle size from 75 to 108 nm.

Among all the surface modifiers, dextran 60, BSA and PEG 1000 at 1% w/w concentration was found to give maximum physical adsorption on surface of lipid nanoparticle. The polydispersity indices were noted for DNP, BNP, PNP were 0.184, 0.192 and 0.188, respectively. An incubation time less than 24 h was not sufficient to carry out physical adsorption and more than 24 h did not result in further particle size increase. Therefore, all experiments of surface modification were performed for 24 h. The surface modified lipid nanoparticles were separated from unbound polymers by high speed centrifugation. As the developed nanoparticles had very narrow particle size distribution range attempt to separate the unbound surface modifier from nanoparticles was not successful. Therefore, it was assumed that the added surface modifier at 1% w/w was entirely adsorbed on the surface of lipid nanoparticle. The developed stavudine NP and SM-NP stored at ambient temperature did not show any sign of instability. All the lipid nanoparticles exhibited excellent syringability and injectability with no sign of clogging or blockage of syringe. The zeta potential in Milli-Q water was observed to be in range of -30.12 to 34 mV. There was not much effect of surface modification on zeta potential confirming that the surface was modified without changing the stability of system. TEM and AFM photomicrograph of the SM-NP confirmed the spherical shape (size between 10 to 300 nm) and can be correlated with particle size obtained with LD and PCS (Figure 1 and 2). In TEM/AFM images, it is possible to observe agglomerates; this could be because of drying step employed during sample preparation. A good reproducibility existed between the two techniques (Figure 1 and 2).

Cellular uptake studies

Effect of incubation time (0.5 to 2h) on the cellular uptake is clearly shown in Figure 3. A stronger fluorescence in the cells as function of incubation time was observed. The enhanced intracellular drug levels could contribute to effective virus killing at various stages of replication. The primary macrophages incubated with STV-DS showed 4% cellular uptake after 120 min. The uptake of stavudine entrapped lipid nanoparticles was time dependent. NP showed uptake of 12% within few minutes as compared STV-DS, resulting in highest fluorescence intensity at 1 h. Phase contrast micrographs also clearly showed that the intensity of nanoparticles was more in nucleus than that of cytoplasm. Fluorescence was not detected in control cells that had not been exposed to the fluorescent nanoparticles.

PEGylation is well reported for avoiding the opsonization [7,23]. Batch PNP showed 22% cellular uptake which was almost 1.83 times more than that of NP and 5.5 times higher than that of STV-NP. The results obtained with PEGylated nanoparticles are contradictory to that reported in literature [7,24]. The larger particle size of PNP (108 nm) as compared to NP (75 nm) could have facilitated endocytosis of nanoparticles. Lipid nanoparticle batch DNP showed 63.72% increase in cellular uptake which was 5.31 times higher than that of NP and 15.93 fold higher than STV-DS. Within 5 min, DNP showed 4.35 fold higher cellular uptake. At all time point, DNP showed very dense nanoparticle distribution inside cytoplasm and nucleus, which was sustained up to 2h, beyond that no increase in intensity was observed, this could be due to saturation of cellular components. Phase contrast micrographs showed slight diffusion of dye out of cell membrane at end of 2h could probably be an indication of release of drug from macrophage cells which plays major role in HIV latency and serve as excellent target for effective drug therapy. As carbohydrates are very essential components of cell systems, surface modification using polysaccharide probably provided suitable surface for interaction with cell receptor and thus could have promoted rapid in cellular uptake with increase in fluorescence intensity over the time. Albumin coated particles (BNP) also showed high cellular uptake within 5 min which was sustained up to 1 hour. At end of 2h, a slight depletion in fluorescence intensity was observed which could be due to release of fluorescent dye. BNP showed highest cellular uptake of 44.28% which was 3.69 fold higher than that of NP and 11.07 fold more than that of STV-DS, within 5 min BNP showed 2.66 times higher cellular uptake as compared to NP which could not be obtained with NP even after 2h incubation. All the SM-NP showed higher cellular uptake as compared to NP. The cellular uptake studies therefore enabled us to understand the interactions of uncoated and surface coated surfaces with cells *in vitro* before their use *in vivo*. The developed stavudine lipid nanoparticles of smaller size of < 108 nm have great potential after surface modification to improve the efficiency of cellular uptake and can be used for cell based antiretroviral drug delivery selectively to macrophage cells (Figure 3).

Cytotoxicity studies

The cytotoxicity of NP was accessed in murine macrophages.

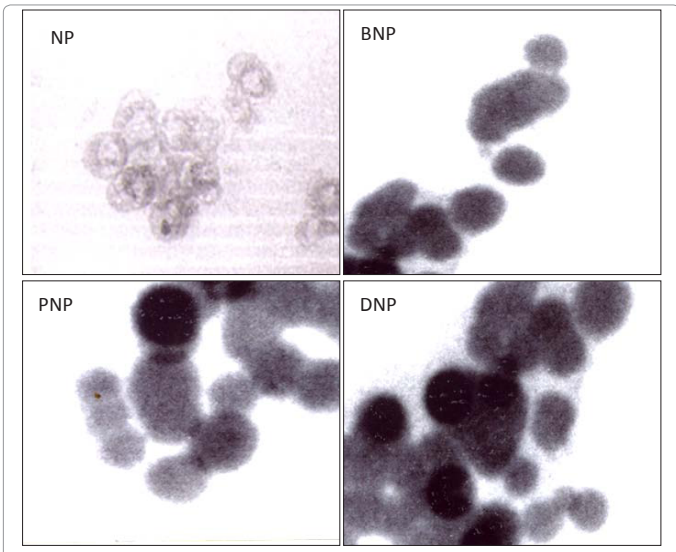

Figure 1: Transmission electron microscopy images of bare and surface modified stavudine lipids nanoparticles.

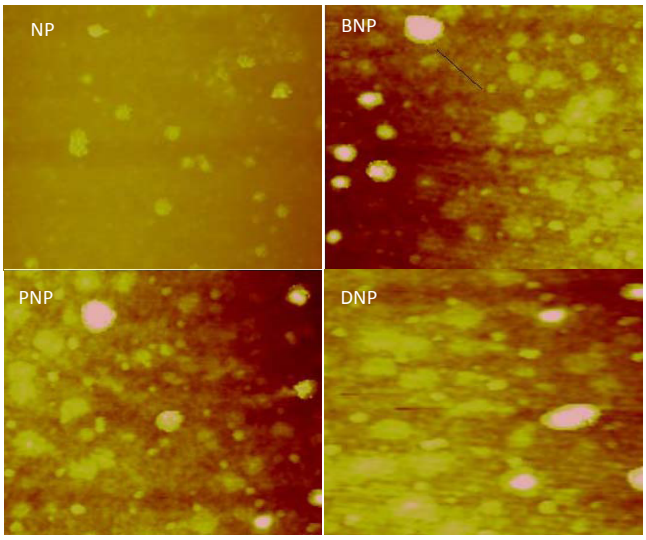

Figure 2: AFM images of bare and surface modified stavudine lipids nanoparticles.

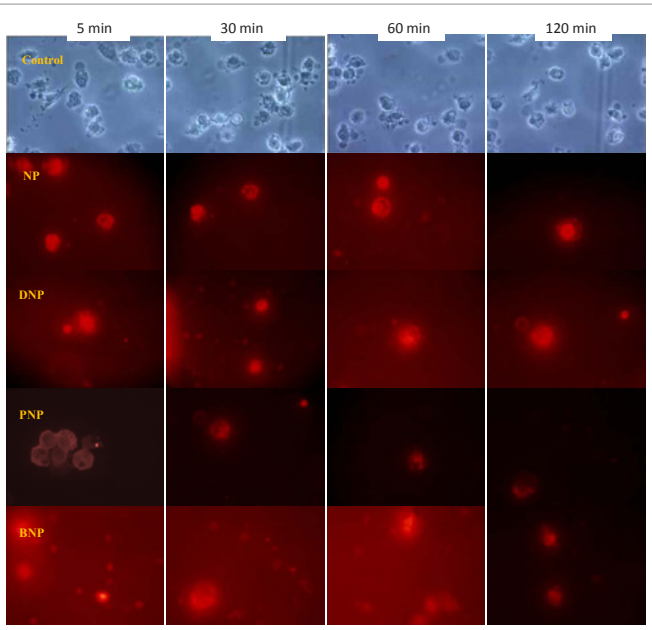

Figure 3: Phagocytic uptake of bare and surface modified stavudine lipids nanoparticles at various time intervals.

High cell viability was observed for STV-DS, NP and SM-NP at low concentration of 0.6µg/ml, the viability was further decreased when concentration was increased up to 1.2µg/ml. The inhibition concentration (IC_{50}) was 0.6µg/ml for NP, BNP and PNP and 1.2µg/ml for DNP. As phagocytic uptake is much higher for NP and SM-NP i.e. high concentration within cell cytoplasm no added toxicity was observed as compared to STV-DS. Therefore, the cytoplasmic transport of nanoparticles can be improved by surface modification without increasing the cytotoxicity (Figure 4).

In vivo studies on stavudine lipid nanoparticles

NP and SM-NP were directly labeled using 99mTc using stannous chloride as a reducing agent. The optimized labeling was obtained

at pH of 7.01 ± 0.11 after 30 minutes of incubation and at 1000 µg/ml concentration of reducing agent. The radiolabelled coated and uncoated lipid nanoparticles showed excellent *in vitro* stability in PBS (pH 7.4) and plasma. An excellent binding affinity of 99mTc to lipid nanoparticles was observed when challenged by DTPA. The NP and SM-NP particles were successfully labeled with technetium and the formed radio complex has excellent stability both at *in vitro* and *in vivo* conditions.

Pharmacokinetics

The radiolabelled NP and SM-NP circulated in blood for longer period of time i.e. beyond 8 h. This is can be further confirmed from prolonged MRT of NP (3.369 h) to STV-DS (2.055 h). SM-NP was cleared from the blood faster as compared to NP. PEGylated nanoparticle batch PNP showed no blood activity at the end of 8h and a short MRT of 1.717h. However, the dextran and BSA coated formulation remained in circulation for longer period of time with MRT of 4.128h and 3.619h, respectively. Both of these formulations were also showed higher bioavailability as indicated by $AUC0_{24}$ as compared STV-DS. The data indicated that lipid nanoparticles were rapidly cleared from the blood compartment to localize to the mononuclear phagocyte system (MPS), particularly to liver and spleen macrophages after IV injection in rat. The *in vivo* behavior of the SM-NP was similar to those NP but with high $AUC0_{24}$ reflecting the localization in the liver and spleen which participate to a major degree in the clearance of particles from the blood. The good labeling stability *in vitro* and *in vivo* suggests that intact particles are being followed (Figure 5).

Gamma imaging

The radio-labelled formulations showed clear body distribution of STV-DS, NP and SM-NP in rat. The placebo and bare nanoparticles were mainly accumulated in RES (reticulo-endothelial) organs and showed that significant radio activity entered in spleen within 30 min. Surface modification of lipid nanoparticles resulted in further enhancement in various organs. Batch BNP, PNP and DNP showed higher accumulation intensities in spleen within 30 min. None of the formulations was able to cross blood brain barrier. Encapsulation of the stavudine in lipid core reduced its excretion through kidney and allowed more deposition in the liver and spleen. The localization of formulations was more prominent between 4 and 8h. The surface modification of nanoparticles helped to enhance accumulation and efficient retention to RES systems as compared to BL-NP and STV-DS.

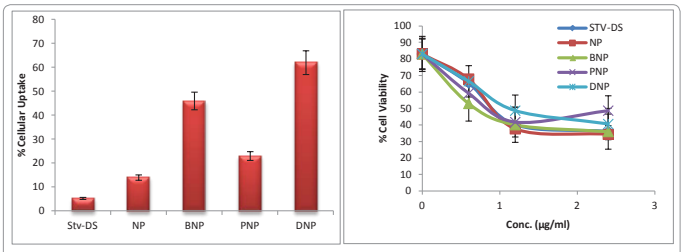

Figure 4: A) Percentage intracellular localization of stavudine bare and surface coated lipid nanoparticles in primary macrophages at end of 2 h B) Cytotoxicity profiles of stavudine lipid nanoparticles when incubated with J744.A12 murine macrophages as determined by MTT assay.

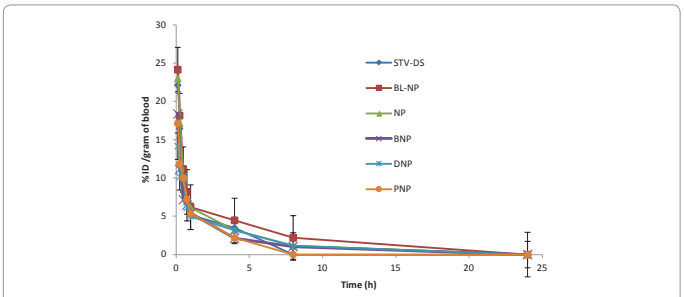

Figure 5: Comparative blood clearance profile of radiolabelled stavudine NP and SM-NP at different time intervals in rats.

Tissue distribution

To know gamma activity in individual tissue, biodistribution studies were carried out. It was found that STV-DS was cleared very rapidly via kidney from blood compartment because of its short biological half-life (0.9-1.2h) [25]. Based on further dissection studies, it was found that none of the formulation as well as pure technetium has crossed blood brain barrier. Similarly, none of the formulation was able to enter thymus which serves as important organ in HIV latency except NP. Slightly higher levels of gamma count were obtained in thymus for technetium as compared with NP which was sustained up to 4h.

Highest $AUC0_{24}$ of 62.88 counts.h/g was obtained for NP followed by DNP (62.74 counts.h/g), PNP (55.838 counts.h/g) and BNP (57.01 counts.h/g) as compared with STV-DS (22.338 counts.h/g) in heart. The MRT was found to be the most prolonged for BNP (11.772 h) followed by DNP (9.877 h) and PNP (4.293 h), respectively. Surface modifications showed increase in gamma count in heart as compared to STV-DS. NP showed 1.46 fold enhancements as compared to STV-DS in gamma count. Surface modification further enhanced it up to 1.58, 1.48 for BNP and DNP, respectively. Batch BNP showed the highest $AUC0_{24}$ of 213.47counts.h/g with comparable MRT as that of bare nanoparticles (~8.6h). NP showed lower MRT (8.674 h) as compared to STV-DS (10.251h). Surface modification of NP resulted in 1.24, 1.85 and 1.63 fold increase in liver gamma count for BNP, DNP and PNP, respectively as compared to NP at the end of 8 h which were maintained up to 24 h with slight reduction. Surface modified batch DNP showed highest $AUC0_{24}$ of 570.62 counts.h/g followed by PNP 540.95 counts.h/g and BNP 425.165 counts.h/g, respectively. All the surface modified batches showed very high radio activity retention in liver with MRT of 15.214, 13.773 and 9.321 h for batches PNP, DNP and BNP, respectively.

Bare nanoparticles increased accumulation of lipid nanoparticles in comparison with pure drug in spleen. Surface modification further enhanced the gamma count by 11.61, 10.50 & 13.21 times higher at the end of 8 h as compared to STV-DS. An increase of 1.40, 1.26 and 1.59 fold in gamma count was observed in comparison to NP for BNP, DNP and PNP, respectively. The MRT was prolonged after surface modification than that of STV-DS. Surface modification further showed increased $AUC0_{24}$ for batch DNP (312.09 counts.h/g) followed by PNP (311.24 counts.h/g) and (287.61 counts.h/g) BNP. The MRT was found to 13.189, 10.640 and 11.661 h for DNP, PNP and BNP, respectively which was almost four times higher to that of STV-DS (Figure 6).

The Liver and spleen cells possess lectin receptors specific for carbohydrates could be probable reason of dextran coated formulations showing higher $AUC0_{24}$ as compared to other uncoated and surface coated formulations. The lipid formulations showed very slow excretion from the body (through kidney) as compared to free

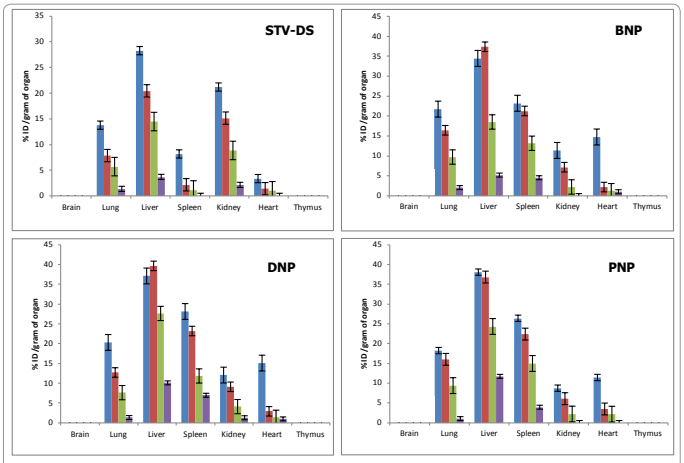

Figure 6: Radioactivity of NP and SM-NP in different rat organs.

drug. The surface modified lipid nanoparticles showed even longer elimination half-life as compared to bare nanoparticles and free drug. Mannose and galactose-specific receptors are present on hepatocytes and kupffer cells, endothelia cells also has mannose receptors [26,27]. The accumulation and retention of carbohydrate-coated systems can be explained on the basis of lectin-carbohydrate interaction. Multi-antenary surface coated systems bind to lectin receptors with more efficiency as the high density of carbohydrates present at their surface increases the probability of lectin carbohydrate interaction and strength of association, the phenomenon called cluster effect. These results are in accordance with the previous reports [28]. The bare and coated lipid nanocarriers rapidly cleared from blood and reached to target MPS rich organs and led to significantly higher drug concentration ($p < 0.05$). Surface coating of these nanoparticles further enhanced its accumulation in liver and spleen, which are potential viral reservoirs in body (Table 1 and 2).

Toxicity assessment

Acute toxicity study showed no signs of abnormal behavioral or physiological changes after dose administration over the observation period of 14 days. No mortality was observed. The food consumption, water intake and weight gain was observed to be within normal ranges. Histological examination of vital tissues indicated no sign of any pathological changes in animals from all the experimental groups as compared with the untreated control group. It was concluded that the STV-DS, NP and DNP as well as the excipients used were absolutely safe at higher dose than that of therapeutic dose level in the experimental animals for acute dose administration. The acute dose toxicity experiment confirmed that at 25 time's higher dose than that of the therapeutic dose of the developed lipid formulations was without any pharmacotoxic signs rendering them pharmacologically safe.

None of the animals from repeated dose toxicity studies showed abnormal behavioral or physiological changes on the day of dose administration and thereafter over the period of 28 days. No mortality has been observed. Histological observation showed some mild degenerative changes in various tissues after repeated administration of the STV-DS, NP and DNP after 28 days. As all anti-retrovirals are well known for their severe toxicity profile, these mild changes are as expected and almost negligible. On the 28th day, liver of the animals receiving STV-DS group showed mild degenerative changes and swelling. The lipid nanoparticulate formulation group showed very insignificant degeneration and proliferation of kupffer cells in the cord and cytoplasm. Mild swellings of tubules were observed in kidney for all the test substances. Minor congestion and hemosidenosis of spleen was seen in all animal groups. Similarly mild congestion and focal pneumonia was evident in the lungs of the animals except the untreated control group. However, it was assumed that before 28th day, most of these degenerative changes might had occurred and slowly vanished indicating restoration of normal function of the tissues. Thus, the histological changes which took place were self limiting and were recovered on discontinuation of the treatment. Therefore, it can be concluded that the all stavudine lipid nanoparticles are well tolerated by rat. Neither of the formulation showed toxicities at a higher dose level administered in a single day. The histological observations on

Time [h]	NP over STV-DS								
Blood	**Lymph**	**Brain**	**Lungs**	**Liver**	**Spleen**	**Kidney**	**Heart**		**Thymus**
1	1.19	1.83	-	1.46	1.15	2.59	0.64	3.30	1.20
4	0.91	3.07	-	1.45	1.23	6.86	0.56	2.64	-
8	1.11	4.45	-	1.09	1.03	8.30	0.42	2.14	-
24	-	-	-	1.22	1.33	1.12	0.53	1.03	-
DNP over NP									
1	0.81	1.52	-	1.01	1.14	1.33	0.88	1.49	-
4	0.99	0.53	-	1.12	1.58	1.57	1.08	0.80	-
8	1.00	1.21	-	1.24	1.85	1.26	1.11	0.53	-
24	-	-	-	0.82	2.44	6.29	1.16	0.97	-
PNP over NP									
1	0.87	0.72	-	0.90	1.17	1.25	0.64	1.12	-
4	0.68	0.53	-	1.40	1.46	1.52	0.71	0.94	-
8	-	0.35	-	1.51	1.63	1.59	0.58	1.00	-
24	-	-	-	0.59	2.81	3.46	-	-	-
BNP over NP									
1	0.88	0.94	-	1.08	1.06	1.10	0.83	1.39	-
4	0.77	0.93	-	1.44	1.48	1.44	0.84	0.59	-
8	0.93	0.79	-	1.57	1.24	1.40	0.59	0.59	-
24	-	-	-	1.32	1.24	4.00	0.01	0.95	-

Table 1: Enhancement in gamma count for SM-NP over NP at various time points.

Tissue	$AUC_{[0-24h]}$	$AUC_{[0-\infty]}$	$AUMC[_{0-24h}]$	MRT
STV-DS				
Blood	23.938	28.811	32.901	2.055
Lungs	122.505	138.382	850.72	10.251
Liver	301.945	344.719	2205.08	10.817
Spleen	35.133	35.136	136.99	3.901
Kidneys	200.60	219.674	1369.38	9.095
Heart	22.338	22.342	105.612	4.473
NP				
Blood	34.566	39.165	76.103	3.369
Lungs	154.955	168.983	1009.84	8.674
Liver	335.555	374.968	2408.54	9.944
Spleen	196.605	205.711	1214.16	7.324
Kidneys	102.81	110.742	656.12	8.153
Heart	62.88	74.196	437.62	11.234
DNP				
Blood	28.985	34.355	72.892	4.128
Lungs	172.45	183.882	1089.42	7.943
Liver	570.62	702.674	4783.7	13.773
Spleen	312.09	381.64	2672.26	13.189
Kidneys	107.58	117.167	730.24	8.799
Heart	62.74	72.763	378.64	9.877
PNP				
Blood	20.829	23.764	25.085	1.717
Lungs	193.415	200.557	1194.52	7.067
Liver	540.95	696.951	4774.02	15.214
Spleen	311.24	352.997	2303.2	10.640
Kidneys	59.973	59.975	273.972	4.569
Heart	55.838	55.841	239.632	4.293
BNP				
Blood	27.529	31.829	62.850	3.619
Lungs	213.47	230.952	1432.2	8.676
Liver	425.165	465.45	3056.72	9.321
Spleen	287.61	335.433	2253.14	11.661
Kidneys	69.268	69.271	296.112	4.276
Heart	57.01	69.849	345.90	11.772

Table 2: Pharmacokinetic parameters of stavudine NP and SM-NP in comparison with STV-DS.

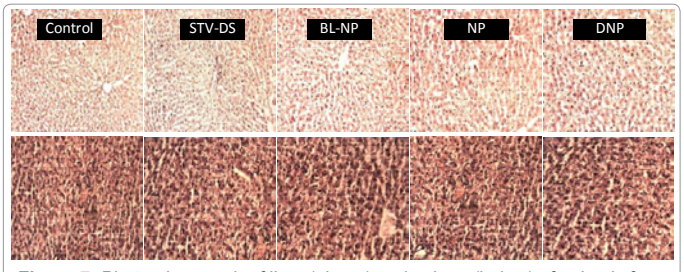

Figure 7: Photomicrograph of liver (above) and spleen (below) of animals from acute toxicity study group.

the 28th day confirmed complete recovery of the animals as evident from absolutely normal condition of the tissues. The developed bare and coated lipid nanoparticles were safe to be administered over the required therapeutic schedule with some mild self limiting pathological changes (Figure 7).

Conclusion

Stavudine entrapped lipid nanoparticles with narrow particle distribution were successfully prepared using high pressure homogenization and their surface was successfully coated with different materials. In this work, we successfully produced lipid nanoparticles and tested their safety and targeting potential *in vivo*. The developed stavudine coated and uncoated lipid nanoparticles have great potential to the limitations in targeting, pharmacokinetics and cellular toxicity posed by conventional drug delivery systems. We have shown that the selective surface coating of nanoparticle is an effective way to achieve cell based targeting particularly in infectious diseases like HIV/AIDS. Further work, is required in optimization of surface coating in terms of surface modifier concentration, layer thickness and stability.

Acknowledgements

Authors would like to thank scientific staff at Bombay veterinary college, Mumbai, India, PERD Research Centre, Ahmedabad, India and KEM Hospital, Mumbai India, for their assistance during carrying out this work. We also thank All India Council of Technical Education (AICTE) for financial support.

References

1. Amiji MM, Vyas TK, Shah LK (2006) Role of nanotechnology in HIV/AIDS treatment: potential to overcome the viral reservoir challenge. Discov Med 6: 157-162.
2. das Neves J, Amiji MM, Bahia MF, Sarmento B (2010) Nanotechnology-based systems for the treatment and prevention of HIV/AIDS. Adv Drug Deliver Rev 62: 458-477.
3. Heiati H, Tawashi R, Shivers RR, Phillips NC (1997) Solid lipid nanoparticles as drug carriers. I. Incorporation and retention of the lipophilic prodrug 3´-azido-3´-deoxythymidine palmitate. Int J Pharm 146: 123-131.
4. Kuo YC, Chen HH (2009) Entrapment and release of saquinavir using novel cationic solid lipid nanoparticles. Int J Pharm 365: 206-213.
5. Chattopadhyay N, Zastre J, Wong HL, Wu XY, Bendayan R (2008) Solid lipid nanoparticles enhance the delivery of the HIV protease inhibitor, atazanavir, by a human brain endothelial cell line. Pharm Res 25: 2262-2271.
6. Gunaseelan S, Gunaseelan K, Deshmukh M, Zhang X, Sinko PJ (2010) Surface modifications of nanocarriers for effective intracellular delivery of anti-HIV drugs. Adv Drug Deliver Rev 62: 518-531.
7. Gref R, Luck M, Quellec P, Marchand M, Dellacherie E, et al. (2000) 'Stealth' corona-core nanoparticles surface modified by polyethylene glycol (PEG): influences of the corona (PEG chain length and surface density) and of the core composition on phagocytic uptake and plasma protein adsorption. Colloids Surf B Biointerfaces 18: 301-313.
8. Stella B, Arpicco S, Peracchia MT, Desmaele D, Hoebeke J, et al. (2000) Design of folic acid-conjugated nanoparticles for drug targeting. J Pharm Sci 89: 1452-1464.
9. Redhead HM, Davis SS, Illum L (2001) Drug delivery in poly (lactide-co-glycolide) nanoparticles surface modified with poloxamer 407 and poloxamine 908: *in vitro* characterisation and in vivo evaluation. J Control Rel 70: 353-363.
10. Goppert TM, Müller RH (2005) Polysorbate-stabilized solid lipid nanoparticles as colloidal carriers for intravenous targeting of drugs to the brain: comparison of plasma protein adsorption patterns. J Drug Target 13: 179-187.
11. Sharma A, Sharma S, Khuller GK (2004) Lectin-functionalized poly (lactide-coglycolide) nanoparticles as oral/aerosolized antitubercular drug carriers for treatment of tuberculosis. J Antimicrob Chemother 54: 761-766.
12. Bakowsky H, Richter T, Kneuer C, Hoekstra D, Rothe U, et al. (2008) Adhesion characteristics and stability assessment of lectin-modified liposomes for site-specific drug delivery. Biochim Biophys Acta 1778: 242-249.
13. van Bilsen PH, Krenning G, Billy D, Duval JL, Huurdeman-Vincent J, et al. (2008) Heparin coating of poly(ethylene terephthalate) decreases hydrophobicity, monocyte/leukocyte interaction and tissue interaction. Colloids Surf B Biointerfaces 67: 46-53.
14. Cavalli R, Bocca C, Miglietta A, Caputo O, Gasco MR (1999) Albumin adsorption on stealth and non-stealth solid lipid nanoparticles. STP Pharma Sci 9: 183-189.

15. Shegokar R, Singh KK (2011) Surface modified nevirapine nanosuspensions for viral reservoir targeting: *In vitro* and in vivo evaluation. Int J Pharm 421: 341-352.

16. Lemarchand C, Gref R, Lesieur S, Hommel H, Vacher B, et al. (2005) Physico-chemical characterization of polysaccharide-coated nanoparticles. J Control Release 108: 97-111.

17. Stahn R, Zeisig R (2000) Cell adhesion inhibition by glycoliposomes: effects of vesicle diameter and ligand density. Tumour Biol 21: 176-186.

18. Clark MA, Hirst BH, Jepson MA (2000) Lectin-mediated mucosal delivery of drugs and microparticles. Adv Drug Deliv Rev 43: 207-223.

19. Shegokar R, Singh KK (2011) Stavudine entrapped lipid nanoparticles for targeting lymphatic HIV reservoirs. Die Pharmazie 66: 264-271.

20. Shegokar R, Singh KK, Muller RH (2011) Production & stability of stavudine solid lipid nanoparticles--from lab to industrial scale. Int J Pharm 416: 461-470.

21. Shegokar R, Singh KK (2011) Conversion of stavudine lipid nanoparticles into dry powder. Int J Pharm Biosci 2: 443-457.

22. Hirata T, Amiya S, Akiya M, Takei O, Sakai T, et al. (2008) Chemical modification of carbon nanotube based bio-nanosensor by plasma activation. Jpn J App Physics 47: 2068-2071.

23. Huang M, Wu W, Qian J, Wan DJ, Wei XL, et al. (2005) Body distribution and in situ evading of phagocytic uptake by macrophages of long-circulating poly (ethylene glycol) cyanoacrylate-co-n-hexadecyl cyanoacrylate nanoparticles. Acta Pharmacol Sin 26: 1512-1518.

24. Wattendorf U, Kreft O, Textor M, Sukhorukov GB, Merkle HP (2008) Stable stealth function for hollow polyelectrolyte microcapsules through a poly(ethylene glycol) grafted polyelectrolyte adlayer. Biomacromolecules 9: 100-108.

25. Kaul S, Dandekar KA, Schilling BE, Barbhaiya RH (1999) Toxicokinetics of 2',3'-didehydro-3'-deoxythymidine, stavudine (D4T). Drug Metab Dispos 27: 1-12.

26. Opanasopit P, Shirashi K, Nishikawa M, Yamashita F, Takakura Y, et al. (2001) In vivo recognition of mannosylated proteins by hepatic mannose receptors and mannan-binding protein. Am J Physiol Gastrointest Liver Physiol 280: G879-889.

27. Agashe HB, Babbar AK, Jain S, Sharma RK, Mishra AK, et al. (2007) Investigations on biodistribution of technetium-99m-labeled carbohydrate-coated poly(propylene imine) dendrimers. Nanomed 3: 120-127.

28. Kao YJ, Juliano RL (1981) Interactions of liposomes with the reticuloendothelial system. Effects of reticuloendothelial blockade on the clearance of large unilamellar vesicles. Biochim Biophys Acta 677: 453-461.